Acta Cryst. (1961). **14**, 292

Parasitic Multiple Bragg Scattering in the Neutron Crystal Spectrometer

By D. A. O'Connor and J. Sosnowski

Institute of Nuclear Research, Warsaw, Poland

(*Received* 18 *February* 1960)

Nuclear-reactor slow-neutron spectra obtained by the use of a crystal monochromator contain a number of irregular fluctuations in the form of inverted peaks, due to fluctuations in the reflectivity of the crystal. It is shown that these fluctuations are due to Bragg reflection of neutrons by reflecting planes other than that used to obtain the monochromatic beam. Approximate formulae are derived for the magnitude and half-width of these inverted peaks for a mosaic crystal. Experiments carried out with copper and aluminium single crystals confirm that the Bragg angles at which the peaks occur depend on the type of crystal structure and not on the lattice constants. The measured depth of the better defined peaks is in satisfactory agreement with that calculated on the basis of the approximate formulae. Comparison of measurements with the crystals at room temperature and liquid-air temperatures failed to reveal the presence of inelastic scattering as a contributory factor to the fluctuations in reflectivity.

Introduction

The curves obtained for the thermal-neutron spectrum of a nuclear reactor, using a crystal monochromator, are known not to be smooth but to contain a large number of small fluctuations. Since the reactor spectrum is known to be a smooth function it must be concluded that the variation of crystal reflectivity with neutron wavelength exhibits small fluctuations corresponding to those observed in the spectrum curves. Spencer & Smith (1959) have shown that for beryllium and sodium chloride crystals, these fluctuations are due to Bragg reflection of neutrons by crystal planes other than the plane being used to obtain the monochromatic beam. Duggal (1959) has suggested that some of the fluctuations in the case of aluminium crystals can be explained as due to inelastic scattering of neutrons of other wavelengths into the monochromatic beam. We give below a simple theoretical treatment of the phenomenon of parastic Bragg reflection in a mosaic crystal and an account of experiments carried out on aluminium and copper crystals.

Theory

Reflection of neutrons by more than one crystal plane in a single crystal will occur when the sphere of reflection intersects more than one lattice point in reciprocal space. In the case of the use of a crystal as a monochromator the conditions under which this will occur are illustrated in Fig. 1. P is the lattice point corresponding to the plane being used to give the monochromatic beam, (referred to later as the principal reflecting plane). Rotation of the crystal in the beam is equivalent in reciprocal space to the movement of the centre of the reflecting sphere along the line RR^1 which lies in the plane of incidence and bisects at right angles the line joining P to the origin. For certain values of the angle θ the sphere of reflection will pass through additional reciprocal lattice points such as P^1 in the figure.

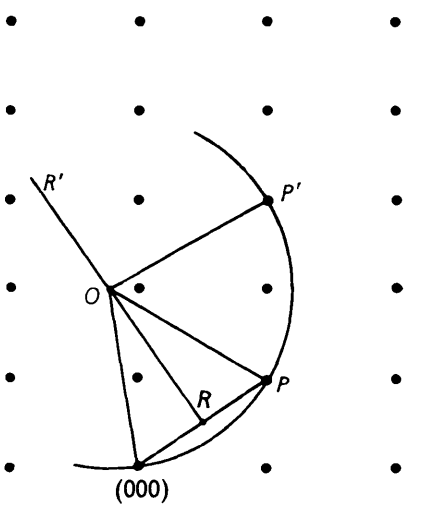

Fig. 1. Construction in reciprocal space illustrating simultaneous Bragg reflection by two planes.

Planes corresponding to such points we shall refer to below as 'parasitic' reflecting planes. Here, for clarity, P^1 has been chosen in the plane of reflection which is also assumed to be a principal symmetry plane of the crystal, but most frequently the additional points will not be in the same plane. To find the values of θ at which multiple Bragg reflection will occur it is necessary to express the coordinates of the point O as functions of θ and then for a given lattice point P' require that $OP=OP'$. The carrying out this calculation for a general case is of little importance but there are some points of interest which can be deduced from the geometry of the problem without calculation. For all crystals of cubic symmetry, and for the same conditions of incidence of the neutron beam, it is

clear that multiple reflections will always occur at the same angles of incidence independently of the value of the lattice constant. Thus in Fig. 1 the angle θ for which the sphere of reflection passes through both P and P' is independent of the scale of the diagram. For other symmetry systems multiple Bragg reflection will occur at the same angles of incidence in crystals which have the same ratios between lattice constants and the same angles between crystal axes. Finally it should be noticed that when multiple Bragg reflection occurs for a first-order reflection then it also occurs for higher-order reflections at the same angles of incidence (e.g. the third order reflection in Fig. 1 will be found by enlarging the sphere of reflection three fold with respect to the reciprocal lattice, θ remaining unchanged).

For an ideal crystal the range of angle of incidence over which multiple Bragg reflection can occur will be of the same order as the angular width of the Bragg diffraction pattern for an ideal crystal, i.e. usually of the order of a few seconds of arc. It follows that the corresponding neutron wavelength range will also be very small, of the order of 10^{-3} Å. In a mosaic crystal on the other hand, multiple Bragg reflection will occur for a much larger range of angle of incidence and wavelength. Thus a neutron of such wavelength and angle of incidende that it can be Bragg reflected by the 'principal' reflecting planes of one mosaic block can also be Bragg reflected by the 'parasitic' reflecting planes of another mosaic block if the angle between these blocks is of the appropriate value, even though the neutron wavelength may not exactly correspond to that which gives multiple reflection in an ideal crystal.

Let us denote by λ_0 a neutron wavelength for which multiple Bragg reflection can occur in an ideal crystal, so that

$$\lambda_0 = 2d_1 \sin \theta_{B1} = 2d_2 \sin \theta_{B2} ,$$

where d_1, d_2, θ_{B1} and θ_{B2} are the reflecting plane spacings and Bragg angles for the principal plane and some parasitic reflecting plane respectively. In the case of a mosaic crystal if a neutron of wavelength λ, approximately equal to λ_0, is incident at an angle $\theta_{B1}+\varphi$ then it can be reflected by the planes of a mosaic block tilted at an angle β_1 to the mean of the mosaic block distribution where β_1 is given by

$$\beta_1 = -\varphi - (\lambda_0 - \lambda)/(2d_1 \cos \theta_{B1}) . \qquad (1)$$

This same neutron can also be reflected by the 'parasitic' reflecting planes of a mosaic block lying at an angle β_2 given by

$$\beta_2 = -K\varphi - (\lambda_0 - \lambda)/(2d_2 \cos \theta_{B2}) , \qquad (2)$$

where the constant K depends on the relative orientation of the principal and parasitic reflecting planes and the plane of reflection and $|K| \leq 1$. From (1) and (2) we obtain a relation between β_1 and β_2:

$$\beta_2 = K_1\beta_1 - (K - K_1)\varphi , \qquad (3)$$

where

$$K_1 = d_1 \cos \theta_{B1}/(d_2 \cos \theta_{B2}) .$$

We shall now calculate the reflecting power of a mosaic crystal for the case of multiple Bragg reflection. We assume that primary extinction within the mosaic blocks and absorption of neutrons by the nuclei of the atoms can be neglected. The angular distribution of mosaic blocks is assumed to be isotropic and of Gaussian form, so that the number of blocks lying at an angle β to the mean of the distribution, is given by

$$W(\beta) = 1/(\eta(2\pi)^{\frac{1}{2}}) . \exp [-\beta^2/(2\eta^2)] ,$$

where η is the standard deviation of the distribution. When we have only one reflecting plane to consider Zachariasen (1945) has shown that the reflectivity of a layer of blocks of thickness dt is equal to σdt where

$$\sigma = QW(\theta - \theta_B)/\gamma \qquad (4)$$

and $\theta - \theta_B$ is the deviation of the angle of incidence from the Bragg angle for the neutron wavelength considered, Q is a function of wavelength and of the reflecting plane spacing, and γ is the direction cosine of the incident beam relative to the inward normal to the crystal face. Bacon & Lowde (1948) have shown that for a non-absorbing mosaic crystal the reflectivity is given by (Bragg case):

$$R(\theta - \theta_B) = \sigma T_0/(1 + \sigma T_0) , \qquad (5)$$

where T_0 is the thickness of the crystal. For multiple Bragg reflections this expression must be modified. We first take the case where there is only one additional parasitic reflecting plane. Expressions of the type (4) will exist for both planes, and using the notation introduced earlier we have for neutrons of wavelength λ incident at an angle $\theta_{B1}+\varphi$:

$$\sigma_1 = (Q_1/\gamma) W(\beta_1)$$

and

$$\sigma_2 = (Q_2/\gamma) W(\beta_2) ,$$

where β_1 and β_2 are given by equations (1) and (3). If $P_0(t)$, $P_{H1}(t)$ and $P_{H2}(t)$ are the powers of the incident and the two reflected beams respectively at a depth t in the crystal then we can write for the Bragg case:

$$\begin{aligned} dP_0(t) &= -(\sigma_1 + \sigma_2)P_0(t) . dt + \sigma_1 P_{H1}(t) . dt + \sigma_2 P_{H2}(t) . dt \\ dP_{H1}(t) &= -\sigma_1 P_0(t) . dt + (\sigma_1 + \sigma') P_{H1}(t) . dt \\ dP_{H2}(t) &= -\sigma_2 P_0(t) . dt + (\sigma_2 + \sigma'') P_{H2}(t) . dt , \end{aligned} \qquad (6)$$

where the cross sections σ' and σ'' represent scattering of the emergent beam P_{H1} by the 'parasitic' reflecting planes of the crystal, and scattering of the P_{H2} beam by the principal reflecting planes. This additional scattering of the emergent P_{H1} beam will not in general be in the same direction as P_{H2} and vice versa. Furthermore it follows from the geometry of the problem that both σ' and σ'' will fall off more rapidly with increase in β_1 than either σ_1 or σ_2, and will there-

fore have much smaller average values. As a first approximation σ' and σ'' can be neglected and equation (6) solved with the boundary conditions $P_{H1}(T_0)=P_{H2}(T_0)=0$. P_0, P_{H1} and P_{H2} have the same form:

$$P(t)=A+B\exp(at)+C\exp(-at),$$

where $a=(\sigma_1\sigma_2)^{\frac{1}{2}}$ and A, B and C are constants, different for the three beams. Applying the boundary conditions, we obtain for the reflectivity of the crystal:

$$R(\beta_1,\beta_2)=\frac{P_{H1}(0)}{P_0(0)}=\frac{a(\cosh aT_0-1)+\sigma_1\sinh aT_0}{a(2\cosh aT_0-1)+(\sigma_1+\sigma_2)\sinh aT_0}. \quad (7)$$

When $(\sigma_1\sigma_2)^{\frac{1}{2}}<T_0^{-1}$ equation (7) reduces to

$$R(\beta_1\beta_2)\sim\sigma_1T_0/(1+(\sigma_1+\sigma_2)T_0). \quad (8)$$

On the other hand, when aT_0 is large and $\sigma_1\gg\sigma_2$, the relative error of the approximate expression (8) is small and approximately given by $(\sigma_2/\sigma_1)^{\frac{1}{2}}$. Comparison of the expressions (8) and (5) suggests that, where there is more than one interfering reflecting plane, the appropriate approximate expression for the reflectivity will be

$$R\sim\sigma_1T_0/[1+(\sigma_1+\sigma_2+\sigma_3+\ldots)T_0]. \quad (9)$$

To obtain an exact solution when there is more than one interfering plane would be possible but the resulting expressions would be even less tractable than (7). In what follows, use will be made of the approximate expression (9).

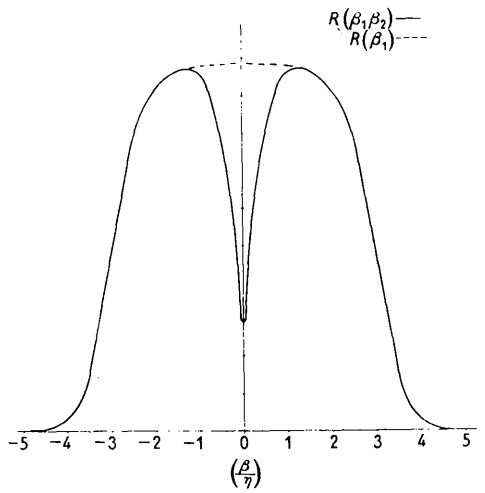

Fig. 2. Reflectivity of a mosaic crystal. $R(\beta_1)$—normal case, $R(\beta_1\beta_2)$—with additional 'parasitic' reflection.

Fig. 2 illustrates the shape of $R(\beta_1\beta_2)$ as a function of β_1 for the case $\lambda=\lambda_0$, $\varphi=0$, where secondary extinction is assumed to be large (i.e. $Q_1\gg 1$), and Q_1, Q_2 have typical values. It is seen that $R(\beta_1\beta_2)$ coincides with $R(\beta_1)$ for large values of β_1 but possesses a dip or 'inverted peak' around $\beta_1=0$. The width of this inverted peak depends on the value of K_1 (equation (3)). If $\lambda\neq\lambda_0$ or $\varphi\neq 0$ then the inverted peak will be shifted to one side of the curve, and if $|\lambda-\lambda_0|$ or $|\varphi|$ are sufficiently large then the anomaly will completely disappear.

The effect of the depression in reflectivity at $\lambda=\lambda_0$ on the intensity of the reflected beam of a crystal monochromator will be to produce a dip in the curve of intensity against wavelength at $\lambda=\lambda_0$. The shape of this inverted peak and its magnitude will depend both on the crystal properties and on the angular resolution of the monochromator. Consider an arrangement consisting of entrance collimator—crystal—exit collimator. The intensity of the monochromatic beam is normally given by (Borst *et al.*, 1953):

$$N=\int_\lambda n(\lambda)d\lambda\int_\alpha I_1(\alpha)I_2(2\beta_1-\alpha)R(\beta_1)d\alpha,$$

where $n(\lambda)d\lambda$ is the number of neutrons in the interval λ—$(\lambda+d\lambda)$, $I_1(\alpha)$ is the transmission of the first collimator for neutrons passing at an angle α (in the plane of the reflection) to the collimator axis and I_2 a similar function for the exit collimator (an instrumental constant is omitted). Assuming $n(\lambda)$ and $R(\beta_1)$ to be slowly varying functions of λ in the range of interest, the expression for N can be rewritten as:

$$N=n(\lambda).2d\cos\theta\int_{\beta_1}\int_\alpha I_1(\alpha)I_2(2\beta_1-\alpha)R(\beta_1)d\alpha d\beta_1, \quad (10)$$

where θ is the angle of reflection.

If at the angle of reflection θ_0 multiple Bragg reflection occurs, then the intensity of the reflected beam at an angle $\theta_0+\psi$, where ψ is small, will be given by

$$N'(\psi)=n(\lambda).2d\cos\theta_0\times\int_{\beta_1}\int_\alpha I_1(\alpha)I_2(2\beta_1-\alpha)R(\beta_1\beta_2\beta_3\ldots)d\alpha d\beta_1, \quad (11)$$

where $R(\beta_1\beta_2\beta_3\ldots)$ is given by equation (9) and $\beta_2\beta_3$ etc. are related to β_1 according to equation (3) where φ is replaced by $\psi-\alpha$. Thus

$$\beta_2=K_1\beta_1-(K-K_1)(\psi-\alpha)$$

and $\beta_3\beta_4$ etc. are given by analogous expressions.

Owing to the form of the expressions for the reflectivity it is not possible to obtain values for the integrals in (10) and (11) analytically. If certain simplifying assumptions are made then some useful approximate formulae can be obtained. It is assumed that the exit and entrance collimators are identical and that their transmission function is given by

$$I(\alpha)=\exp[-\alpha^2/(2\Phi^2)].$$

Consider the simple case of a single interfering parasitic reflection. If $Q_2/Q_1<1$ then from equations (5) and (8) we obtain for the depression in reflectivity

$$R(\beta_1)-R(\beta_1\beta_2)\sim R(\beta_1)Q_1W(\beta_1)/Q_2W(\beta_2). \quad (12)$$

If $Q \gg 1$ then $R(\beta_1)$ can be approximately represented by a step function of the form

$$R=1,\ |\beta_1| \leq \beta_0;\quad R=0,\ |\beta| \geq \beta_0\,,$$

where

$$\beta_0 = \eta\left(2\ln\frac{Q_1 T_0}{(2\pi)^{\frac{1}{2}}\gamma\eta}\right)^{\frac{1}{2}}.$$

Then from (10), (11), and (12) we obtain

$$N-N'(0) = 2d_1\cos\theta_0 . n(\lambda)(Q_2/Q_1) \times \int_{-\beta_0}^{\beta_0}\int_{-\infty}^{\infty} I_1(\alpha)I_2(2\beta_1-\alpha)(W(\beta_2)/W(\beta_1)d\alpha\, d\beta_1)$$

and

$$N = 2d_1\cos\theta_0 n(\lambda)\int_{-\beta_0}^{\beta_0}\int_{-\infty}^{\infty} I_1(\alpha)I_2(2\beta_1-\alpha)d\alpha\, d\beta_1\,.$$

Integration of these expressions yields

$$(N-N'(0))/N \sim (Q_2/Q_1)(1+K_1^2\Phi^2/(2\eta^2))^{\frac{1}{2}}. \quad (13)$$

This is the maximum fractional drop in intensity of the reflected beam caused by a single parasitic reflection. Where there is more than one parasitic reflecting plane then the appropriate approximate expression will be given by the sum of the appropriate number of expressions of the type (13).

The half width of an inverted peak can be estimated in the following way. When Q_1 is very large (strong secondary extinction) it follows from equation (8) that the area of the dip in the reflectivity curve is relatively independent of the position of the dip on the curve. It should be further noted that the half width of this dip is at least K_1 times smaller than the width of the $R(\beta_1)$ curve, (this follows from equation (3)) and in practice K_1 is found usually to be greater than 3. The position of the dip is found by putting $\beta_2=0$ in equation (3) which gives

$$\beta_1' = ((K-K_1)/K_1)(\psi-\alpha)\,.$$

It follows that the contribution of this drop in reflectivity to the drop in reflected intensity will be proportional to

$$N-N'(\psi) \sim \text{const.}\int_{-\infty}^{\infty} I_1(\alpha)I_2(2\beta_1'-\alpha)d\alpha\,.$$

Integration gives

$$N-N'(\psi) \sim \text{const.}\exp\left[-\psi^2/5\Phi^2\right]. \quad (14)$$

From (13) and (14) it is seen that, when secondary extinction is strong, the half-width of an inverted peak is porportional to the half-width of the collimator function and that the depth of an inverted peak is approximately proportional to the reciprocal of the collimator half-width. It follows that the area of an inverted peak is approximately independent of the collimator width (assuming of course that all the approximations made here are justified). From (14) it also follows that the depth of an inverted peak is proportional to the mosaic spread. This is explained by the fact that an increase in the mosaic spread gives an increase in the range of angles of incidence over which simultaneous reflection by several reflecting planes can occur.

Experiments

Measurements were made of the variation of reflected neutron intensity with wavelength for copper and aluminium single crystals in the range of Bragg angle of 10° to 35°. The universal double-crystal spectrometer at the WWRS reactor in Warsaw was used. The collimators were of nominal half-angle 10 min. The crystals were half-cylindrical in cross-section, of approximate thickness 2 cm. and exposed reflecting surfaces of dimensions 5×4 cm. Both for copper and aluminium the (111) reflecting planes were used and the plane of incidence was $(\bar{1}10)$. Measurements of the intensity were made at angular intervals of 4 min. of arc. Intensity measurements were reproducible to better than 0·5% and the background counting rate was everywhere less than 1% of the intensity of the reflected beam. In order to detect the presence of inelastic scattering effects measurements were repeated on both crystals at the temperature of liquid air (by simply immersing the crystals in the liquid air). Immersion in liquid air produced no change in mosaic structure which could be observed in the crystal rocking curves.

Results and discussion

The curves of reflected neutron intensity versus wavelength obtained for the (111) planes of copper and aluminium crystals are given in Fig. 3. The general shape of the curves depends on the reactor slow-neutron spectrum and the variation of crystal reflectivity and neutron detector efficiency with neutron wavelength. The curves are seen to contain a large number of inverted peaks. As shown in Fig. 3 and in Table 1 the angular positions of the majority of peaks agree with those calculated on the assumption that the inverted peaks are caused by parasitic reflections. Not all of the peaks were identified, presumably because not all of the possible combinations of *hkl* values were utilized in the calculations. In the figure only one *hkl* value is given for each peak but in fact there is always more than one possible combination due to the symmetry of the crystal lattice. It is seen that while the angular positions of inverted peaks are the same for both aluminium and copper the relative depths of some of the peaks are different for the two crystals.

The effect of lowering the temperature of the crystals is convincing evidence of the elastic-scattering origin of the irregularities. For copper, Debye temperature 315 °K., at the temperature of liquid air all the inverted peaks are more pronounced and deeper (relative to the height of the curve between the peaks) than at room temperature, due to the operation of the

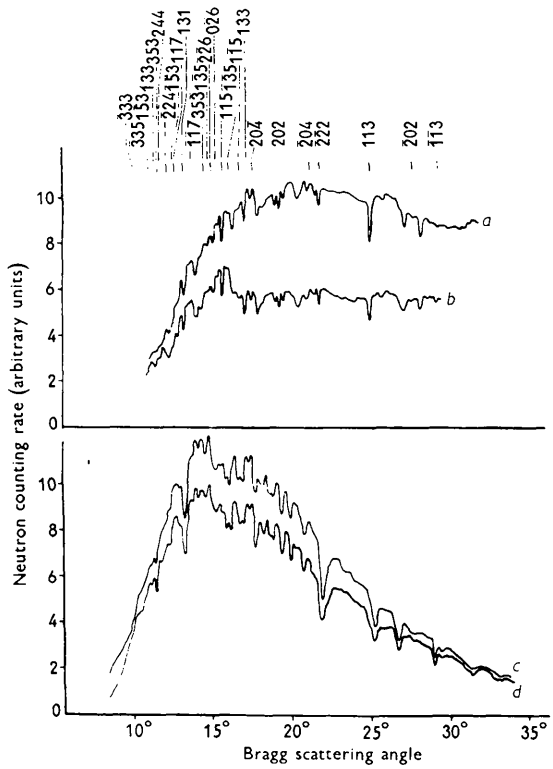

Fig. 3. Uncorrected reactor slow neutron spectra obtained with a crystal monochromator.

a–Cu (111), plane of incidence ($\bar{1}10$), 300 °K.
b–Cu (111), plane of incidence ($\bar{1}10$), ~ 120
c–Al (111), plane of incidence ($\bar{1}10$), 300
d–Al (111), plane of incidence ($\bar{1}10$), ~ 120

Debye–Waller temperature factor. In aluminium this effect is not so marked since its Debye temperature is higher (398 °K.). Not one of the inverted peaks is shallower at the lower temperature. The difference in overall shape between the curves at room and liquid-air temperatures is due to the variation with wavelength of the absorption and scattering of neutrons in the liquid-air and Dewar vessel.

The measured half-width of the well developed and symmetrical inverted peaks was found to agree with the value calculated on the basis of equation (14) within the limits of the experimental error. From previous measurements (O'Connor & Sosnowski, 1959), $\Phi = 5{\cdot}6 \pm 0{\cdot}15$ min., which gives for the half-width of the inverted peaks a value of $21{\cdot}0 \pm 0{\cdot}6$ min. The measured values are given in Table 1. In determining the half-widths the depths of peaks were measured relative to the adjacent unperturbed portions of the curve. Where the measured half-width was larger, the inverted peak is less symmetrical in shape presumably because of the superposition or overlapping of neighbouring peaks.

For the copper crystal at normal temperature the depth of some of the well defined peaks was calculated using the approximate formulae given earlier. The mosaic spread of the copper crystal and the higher-order content of the monochromatic beam for this crystal are known from previous measurements (O'Connor & Sosnowski, 1959). The values calculated using equation (13) are given in Table 2 together with the measured values. The agreement is satisfactory considering the approximations made in the formulae. For one of the peaks, that due to the 113 and 004, a second value was obtained by graphical integration of the integrals in equations (10) and (11). The second order for this wavelength was also taken into account. Again the agreement with the measured value is good

Table 1. *Half-width values*

Typical interfering reflecting plane *hkl*	Calculated Bragg angle	Copper (111)		Aluminium (111)	
		Observed angle	Half width	Observed angle	Half width
($\bar{3}\bar{3}5$)	10° 32′	10° 36′	—	10° 27′	—
($1\bar{5}3$)	11° 7′	—	—	11° 5′	—
($\bar{1}\bar{3}3$)	11° 25′	11° 26′	—	11° 22′	20′
($2\bar{4}4$)	11° 45′	11° 43′	—	—	—
($\bar{1}17$)	12° 41′	12° 51′	—	12° 49′	—
(131)	13° 16′	13° 14′	17′	13° 16′	25′
($1\bar{1}7$)	13° 49′	13° 57′	30′	13° 43′	—
($3\bar{5}3$)	14° 36′	14° 42′	—	14° 33′	20′
($2\bar{2}6$)	15° 4′	15° 9′	26′	15° 9′	—
($0\bar{2}6$)	15° 23′	15° 24′	—	15° 31′	—
($11\bar{5}$)	15° 48′	15° 41′	17′	15° 48′	—
($\bar{1}35$)	16° 14′	16° 24′	34′	16° 31′	—
(204)	16° 52′	16° 47′	—	16° 53′	—
($1\bar{3}3$)	17° 27′	17° 9′	22′	17° 15′	—
(024)	17° 49′	17° 32′	19′	17° 37′	17′
($11\bar{5}$)	19° 28′	19° 23′	15′	19° 23′	20′
($2\bar{2}2$)	22° 0′	21° 54′	19′	22° 0′	46′
($11\bar{3}$)	25° 14′	25° 9′	19′	25° 13′	25′
($\bar{1}\bar{1}3$)	29° 30′	29° 23′	—	29° 29′	—

Half-width values are not given for very shallow inverted peaks for which the half width could not be determined with any certainty. The probable error in half width determinations is ±2′.

(see Table 2). Calculations were not performed for aluminium since its rocking curve showed the existence of two peaks in the mosaic block distribution a few minutes of arc apart.

Table 2.

Interfering reflecting planes	$[(N-N'(0))/N] \times 100$ for copper (111) Measured	Calculated
(115) ($\bar{3}\bar{3}3$) ($\bar{2}\bar{2}4$) ($2\bar{2}4$)	14·5	17·5
(113) (004)	23·5	21·5 (23·0)
($1\bar{3}3$) ($\bar{3}13$)	13·0	13·0
($\bar{2}\bar{2}2$)	9·4	11·4

Calculated values obtained using equation (16). Values in brackets for (113) and (004) obtained by graphical intergration of equations (12) and (13).

Finally it should be pointed out that the density of inverted peaks and their magnitude effectively prohibit the use of the crystal monochromator for precise measurements of neutron spectra. There would appear to be no simple valid method of correcting for these effects. Suitable choice of reflecting plane and plane of reflection could result in a reduction of the number of peaks observed.

References

BACON, G. E. & LOWDE, R. D. (1948). *Acta Cryst.* **1**, 303.

BORST, L. B. & SAILOR, V. L. (1953). *Rev. Sci. Instrum.* **24**, 141.

DUGGAL, V. P. (1959). *Nuclear Sci. and Eng.* **6**, 76.

O'CONNOR, D. A. & SOSNOWSKI, J. Report No. 98/I-B, Institute of Nuclear Research, Warsaw.

SPENCER, R. R. & SMITH, J. R. (1959). *Bull. Amer. Phys. Soc.* Ser. II, **4**, 245.

ZACHARIASEN, W. H. (1945). *X-ray Diffraction in Crystals*. New York: Wiley.

Acta Cryst. (1961). **14**, 297

Diffusion Centrale des Rayons X par des Particules Filiformes

BY V. LUZZATI ET H. BENOIT

Centre de Recherches sur les Macromolécules, 6, rue Boussingault, Strasbourg, France

(*Reçu le 2 avril* 1960)

The asymptotic form of the intensity scattered by an assembly of filiform particles is determined for large values of s and the geometrical parameters it depends on are given.

The influence of certain types of configuration on this asymptotic behaviour is discussed.

Introduction

Le problème mathématique que nous traitons ici nous a été suggéré par l'analyse de données expérimentales, tant de diffusion centrale des rayons X, que de diffusion de la lumière, obtenues avec des solutions de particules longues et rigides, notamment d'acide désoxyribonucléique et de certains polypeptides de synthèse. Bien souvent, en effet, nous avons constaté d'une part que la fonction $i(s)$ expérimentale a, pour s grand, la forme typique de bâtonnets:

$$\underset{s\to\infty}{i(s)} = Ks^{-1} \qquad (1)$$

(K est une constante, $s=2\sin\theta.\lambda^{-1}$, 2θ étant l'angle de diffusion), mais d'autre part que l'écart entre $i(s)$ et sa forme asymptotique Ks^{-1} devient parfois important à mesure que l'on se rapproche des petites valeurs de s.

Or on sait que si un échantillon est formé de bâtonnets longs et rigides, $i(s)$ admet un développement asymptotique dont le premier terme, d'ordre s^{-1}, ne dépend que de leur masse linéaire spécifique (Kratky, 1956; Luzzati, 1960). Nous nous sommes proposé d'étendre ce développement asymptotique en déterminant les paramètres structuraux dont dépendent les termes d'ordre supérieur à s^{-1}. Pour cela nous avons choisi un modèle plus général que celui des bâtonnets, mais dans lequel la matière est toujours distribuée uniformément le long d'un fil.

Ce modèle est analogue à la 'worm-like chain' dont Porod (1949) s'est servi pour traiter un problème analogue à celui que nous nous proposons de résoudre ici: nous discuterons plus loin ses résultats.

Bien que le traitement mathématique soit formulé ici dans le cas de la diffusion des rayons X, il s'applique également à la diffusion de la lumière.

Traitement mathématique

Nous admettons dans la suite que toute la matière de l'échantillon est localisée dans un ou plusieurs filaments de dimensions transversales négligeables, dont la masse spécifique linéaire est partout la même. L est la longueur totale des filaments de l'échantillon, M leur masse ($\mu=M/L$). Nous supposons en outre que l'échantillon est isotrope.